Journal of Luminescence 193 (2018) 61–69

Contents lists available at ScienceDirect

Journal of Luminescence

journal homepage: www.elsevier.com/locate/jlumin

# Transparent oxyfluoride glass-ceramics with $NaGdF_4$ nanocrystals doped with $Pr^{3+}$ and $Pr^{3+}$-$Yb^{3+}$

J.J. Velázquez[a], R. Balda[b,c], J. Fernández[b,c,*], G. Gorni[a], L. Pascual[d], G. Chen[e], M. Sundararajan[e], A. Durán[a], M.J. Pascual[a]

[a] Instituto de Cerámica y Vidrio-CSIC, C/ Kelsen 5, 28049 Madrid, Spain
[b] Applied Physic Department I, Superior school of Engineering, Pais Vasco University, UPV-EHU, Bilbao, Spain
[c] Materials Physics Center CSIC-UPV/EHU, San Sebastian, Spain
[d] Instituto de Catálisis y Petroleoquímica-CSIC, 28049 Madrid, Spain
[e] Department of Physics and Astronomy, Ohio University, Athens OH45701,USA

ARTICLE INFO

*Keywords:*
Glass ceramics
Oxyfluoride
$Pr^{3+}/Yb^{3+}$ codoping
Energy transfer
Downconversion

ABSTRACT

Transparent oxyfluoride nano-glass-ceramics (GCs) containing $NaGdF_4$ nanocrystals doped with $0.1Pr^{3+}$and $0.5Pr^{3+}$, and co-doped with $0.5Pr^{3+}$-$2Yb^{3+}$ ions (mol%) were obtained by melting-quenching followed by heat treatments at temperatures near $T_g$. The addition of rare-earths (RE) ions affects the crystallization kinetics due to the progressive increase of $T_g$ as RE concentration increases. X-ray diffraction (XRD) and high-resolution transmission electron microscopy (HRTEM) show the precipitation of $NaGdF_4$ nanocrystals with sizes between 9 and 30 nm. The crystal size increases with the increasing amount of dopant. Energy dispersive X-ray (EDX) analysis confirms the incorporation of the RE ions in the fluoride nanocrystals in the glass-ceramics. This incorporation is also supported by optical characterization. Photoluminescence measurements shows a better resolved structure together with a narrowing of the $Pr^{3+}$ emission and excitation spectra in the glass–ceramics compared to the precursor glass. The emission spectra and fluorescence decay curves from the $^3P_0$ level of $Pr^{3+}$ in the codoped samples support the existence of a $Pr^{3+} \rightarrow Yb^{3+}$ energy transfer with slight enhancement of the energy transfer efficiency in the GC sample.

## 1. Introduction

Rare-earth (RE) doped nanostructured materials have gained increasing interest in the last decades due to their potential applications in the area of photonic devices. The small size of nanoparticles along with the appropriate choice of host matrix and RE doping improve the luminescent properties opening the way to their use in optical telecommunications, solid state lasers, three-dimensional full-color displays, solar cells, and others [1–5].

Transparent oxyfluoride glass-ceramics containing RE doped fluoride nanocrystals present potential applications in the field of solid-state luminescence. These materials combine the good mechanical and chemical stabilities of oxide glasses with the low phonon energy of fluoride crystals (300–400 $cm^{-1}$), which prevents non-radiative losses by multiphonon relaxation [6–8]. Glass-ceramics can be obtained by an adequate heat treatment of the precursor glass to precipitate, within the glass matrix, nanocrystalline particles of size between 10 and 40 nm. Due to the small particle size the Rayleigh scattering is rather weak and the transparency of these materials is maintained after crystallization [9,10]. Moreover, in oxyfluoride GCs, the RE ions can be effectively hosted in the nanocrystals [11–15], through a diffusion-controlled process, highly dependent on the temperature. Thus, a precise control of the crystallization process is necessary to obtain the highest luminescence efficiency.

Another important issue is the selection of the adequate fluoride matrix for a specific application. Especially, sodium lanthanide tetrafluorides, $NaREF_4$, with Gd, Y, La or Lu, as RE, have been reported to be the ideal luminescence hosts for $Ln^{3+}$ activators and being widely studied. In particular, the crystallization mechanism of these fluoride phases, $NaYF_4$, $NaLaF_4$, $KLaF_4$, and $NaLuF_4$ [5,16–18], in aluminosilicate glasses is shown to occur via regions enriched in Si-, F-, La-, Y- or Lu- and Si-phase separation in the glass, from which the fluoride crystals develop during the heat treatment. The interface between the glass matrix and the crystals in the de-mixed areas is enriched in network formers, mainly $SiO_2$, creating a viscous barrier, which prevents further crystal growth and limits the crystal size to the nanometric range. Moreover La-, Y- and Lu- can be substituted by RE ions after doping. As a result, luminescence properties are enhanced considerable when

---

[*] Corresponding author at: Applied Physic Department I, Superior school of Engineering, Pais Vasco University, UPV-EHU, Bilbao, Spain.
*E-mail address:* joaquin.fernandez@ehu.eus (J. Fernández).

http://dx.doi.org/10.1016/j.jlumin.2017.07.034
Received 28 April 2017; Received in revised form 11 July 2017; Accepted 17 July 2017

compared with the base glass.

Among the different $NaREF_4$ fluoride matrices, sodium gadolinium tetrafluoride ($NaGdF_4$) has been reported to be one of the best converter hosts for $Ln^{3+}$ ions couples, such as $Yb^{3+}$-$RE^{3+}$ [19–23]. In fact, $NaGdF_4$ presents cubic (α) and hexagonal (β) crystalline structures; the luminescence efficiency of $Ln^{3+}$-doped in this host being higher in the β-$NaGdF_4$ phase respect of the α phase [24–26]. Recently, a few reports related to the synthesis, processing and optical properties of the β-$NaGdF_4$ based glass-ceramics have been published. The precipitation of $NaGdF_4$ nanocrystals in glass and the optical properties using $Sm^{3+}$ as structural probe were studied by Andreas Herrmann et al. [27], which concluding that the increase of the Na/Gd ratio favours the crystallization of the β-$NaGdF_4$ phase and enhances the optical properties of $Sm^{3+}$ ions respect to the cubic phase. On the other hand, the relationship between structural and optical properties has been investigated by different authors [28,29] focusing on up-conversion (UC) mechanisms of $Er^{3+}$ and $Er^{3+}$-$Yb^{3+}$ doped β-$NaGdF_4$ GCs; they concluded that the UC luminescent intensity of the glass ceramic is several times stronger respecting to the precursor glass due to the incorporation of $Er^{3+}/Yb^{3+}$ ions into the nanocrystalline phase.

Among lanthanide ions, $Pr^{3+}$ is an important optical activator which offers the possibility of simultaneous blue, green, and red UC emissions for laser action as well as infrared (IR) emission for optical amplification at 1.3 μm [30–32]. Moreover, the $Yb^{3+}$–$Pr^{3+}$ system has received large attention because of the efficient energy transfer processes from $Yb^{3+}$ to $Pr^{3+}$ ions which give rise to up-conversion luminescence and/or IR emission by quantum cutting processes [33–37].

In this work, the crystallization mechanism and the structural and optical properties of $Pr^{3+}$-doped and $Pr^{3+}$-$Yb^{3+}$-codoped $NaGdF_4$ GCs are reported. In particular, the effect of $RE^{3+}$ ions on the crystallization kinetics has been analyzed. The luminescent features of the emission and excitation spectra of $Pr^{3+}$ in the GCs support the incorporation of RE ions into the fluoride nanocrystals. The energy transfer between $Pr^{3+}$ and $Yb^{3+}$ ions is confirmed by the temporal behaviour of the luminescence of $Pr^{3+}$ ions as well as by the presence of the $Yb^{3+}$ emission ($^2F_{5/2} \rightarrow {}^2F_{7/2}$) after 444 nm excitation in the codoped samples.

## 2. Experimental

### 2.1. Materials preparation

Glasses with composition $70SiO_2$-$7Al_2O_3$-$8Na_2O$-$8K_2O$-$7GdF_3$-$xPrF_3$–$yYbF_3$ (70Si-7Gd) doped with $x = 0.1$, 0.5 and 3 and $y = 0$ and 2 (in mol%) have been prepared by the melting-quenching method. The raw materials used were $SiO_2$ (Saint-Gobain, 99.6%), $Al_2O_3$ (Panreac), $Na_2CO_3$ (Sigma-Aldrich, 99.5%), $K_2CO_3$ (Scharlau, 99.99%), $GdF_3$ (Alfa Aesar, 99.9%), $PrF_3$ (Alfa Aesar, 99.9895%), and $YbF_3$ (Alfa Aesar, 99.999%). The batches were calcined at 1200 °C for 2 h and melted at 1600 °C for 1 h and then quenched on a brass mold. The melting process was repeated twice in order to improve the glass homogeneity. The glasses were annealed at 515 °C for 30 min for stress relaxation. Glass pieces were heat treated at 520, 550, 580 and 600 °C during 5 ÷ 120 h, using a heating rate of 10 °C/min in order to get the corresponding glass-ceramics. Polished glass sheets (1 cm × 1 cm × 2 mm), heat treated at 550 °C during 80 were selected for optical characterization. One sheet of base glass for each composition was also used for comparison purposes with the corresponding glass-ceramics.

### 2.2. Thermal and structural characterization

Glass transition temperature ($T_g$), softening point ($T_d$) and thermal expansion coefficient (α) were determined by dilatometry using a Netzsch Gerätebau dilatometer, model 402 PC/1 with a heating rate of 5 °C/min in air; the estimated error of $T_g$ is ± 2 °C.

XRD measurements have been performed with an X-ray diffractometer D8 ADVANCE (Bruker) equipped with a Lynx Eye detector. The patterns were collected with monochromatic CuK$\alpha_1$ radiation (1.54056 Å) in the $10 \le 2\theta \le 70°$ range with steps of 0.02° and 1 s acquisition for each step.

TEM samples of glasses and glass-ceramics were prepared using sieved powders of size < 63 μm. High resolution electron microscopy (HR-TEM), including scanning transmission microscopy-high angle annular dark field (STEM-HAADF) and X-ray energy dispersive spectroscopy (EDXS), were recorded on a JEOL 2100 field emission gun transmission electron microscope operating at 200 kV and providing a point resolution of 0.19 nm. The TEM is equipped with an EDXS energy dispersive X-ray spectrometer (INCA x-sight, Oxford Instruments). EDX analysis was performed in STEM mode, with a probe size of 1 nm. Samples were prepared by dispersing the fine powder, obtained by grinding the glass and GCs pieces, in ethanol with ultrasonic agitation; a droplet of the suspension was put on a copper holey carbon grid.

Small-angle X-ray scattering (SAXS) measurements were performed using a commercial SAXS system (SAXSess, Anton Paar GmbH). The bulk samples were crushed into fine powders and then compressed into uniform thin pellets for SAXS measurements. A Cu Kα line beam of 10 mm × 0.4 mm in size was incident on the samples, and the scattered X-rays were collected using an imaging plate in the q range of 0.01–0.1 Å$^{-1}$. The collected 2D patterns were converted into 1D patterns and desmeared using the line beam profile. The 1D SAXS data were then analyzed using the Irena software package [38] to obtain the particles size distribution.

### 2.3. Optical properties

UV–Vis absorption spectra of optical slabs were measured in the 300–1000 nm range using a Lamba 900-Perkin Elmer double beam spectrophotometer.

Emission and excitation spectra were recorded by using a FLS900 fluorescence spectrometer (Edinburgh Instruments Ltd, UK) equipped with a 450 W Xenon lamp. The emission was detected by Hamamatsu R928P and liquid nitrogen cooled Hamamatsu R5509-72 photomultipliers in the 470–750 nm and 650–1150 nm ranges respectively.

Lifetime measurements were obtained by exciting the samples with a dye laser pumped by a pulsed nitrogen laser, and detecting the emission with a Hamamatsu R636 photomultiplier. Data were processed by a Tektronix oscilloscope. All measurements were performed at room temperature.

## 3. Results and discussion

### 3.1. Thermal and structural properties

Thermal characterization using dilatometry permits obtain the glass

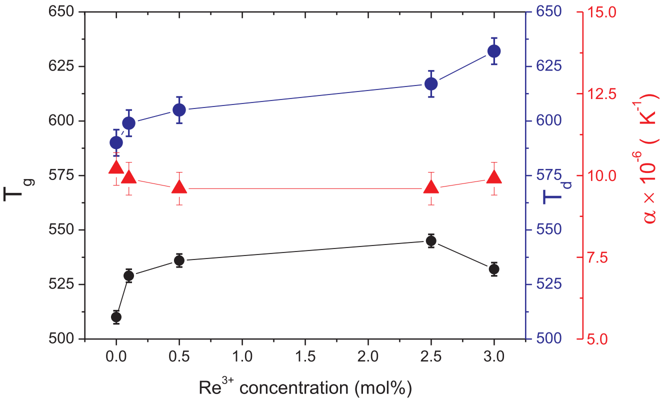

**Fig. 1.** Glass transition temperature ($T_g$) (black), dilatometric softening temperature ($T_d$) (blue), and TEC α (red), versus $RE^{3+}$ concentration (mol%.).